



Use of a rhodamine-based chelator in a microfluidic paper-based analytical device for the *in-situ* copper quantification in natural waters

Juliana I.S. Aguiar^a, Susana O. Ribeiro^b, Andreia Leite^b, Maria Rangel^c,
António O.S.S. Rangel^a, Raquel B.R. Mesquita^{a,*}

^a Universidade Católica Portuguesa, CBQF – Centro de Biotecnologia e Química Fina – Laboratório Associado, Escola Superior de Biotecnologia, Rua Diogo Botelho 1327, 4169-005, Porto, Portugal

^b Universidade do Porto, Faculdade de Ciências, Departamento de Química e Bioquímica, REQUIMTE-LAQV, 4169-007, Porto, Portugal

^c Universidade do Porto, Instituto de Ciências Biomédicas de Abel Salazar, REQUIMTE-LAQV, 4050-313, Porto, Portugal

ARTICLE INFO

Handling editor: J.-M. Kauffmann

Keywords:

Copper(II) determination
Functionalized copper ligand
In-situ analysis
Natural waters
Paper sensor device

ABSTRACT

This work describes the development of a microfluidic paper-based analytical device (μ PAD) for the determination of copper in fresh and marine waters. A functionalized rhodamine-based chelator was synthesized and used as a chromogenic reagent, forming a highly intense pink complex with the analyte. The aim was to create a paper device that offers optimal performance and provides *in-situ*, rapid and cost-effective analysis in line with World Health Organization guidelines. The influence on the determination of several physical and chemical parameters was evaluated aiming to achieve the best performance. Under optimised conditions, a linear correlation was established in the range of 0.05–0.50 mg L⁻¹ of copper, with a limit of detection of 10 μ g L⁻¹. The accuracy of the proposed method was assessed by comparing the results obtained with the developed μ PAD and the results obtained with Inductively Coupled Plasma measurements (RE < 10 %). Recovery studies were also performed using different types of water samples with no need for any prior sample pre-treatment: tap, well, river and seawater. The average recovery percentage of 101 % (RSD = 4.3 %) was obtained, a clear indication of no multiplicative matrix interferences.

1. Introduction

Copper is an abundant trace element in the environment and an essential micronutrient for most living organisms [1–3]. However, when present at high levels, copper is listed as a priority pollutant by the United States Environmental Protection Agency (US-EPA) due to its potential negative effects on aquatic ecosystems [4]. When people are exposed to excess amounts of copper, by drinking contaminated water or consuming contaminated food, it can be harmful to human health (kidney or liver damage, gastrointestinal problems, and neurodegenerative diseases) [5,6]. To ensure public safety, US-EPA has set the limit for Cu²⁺ in drinking water at 1300 μ g L⁻¹ [7].

Conventionally, inductively coupled plasma-mass spectrometry (ICP-MS) or atomic absorption spectrometry (AAS) have been the primary laboratory-based techniques used for copper assessment in water samples. These techniques offer high analytical performance in terms of sensitivity, specificity, and precision. However, they require sophisticated instrumentation and trained operators, leading to significant

analysis cost [8]. To overcome some of these limitations, the development of rapid and point-of-care testing methods based on low-cost detection technologies has been a researcher's target.

In this context, microfluidic paper-based analytical devices (μ PADs) can be an effective alternative approach for water quality assessment [9–11]. Paper-based devices are easy to fabricate, user-friendly and less expensive, compared to conventional techniques. Moreover, μ PADs enable *in-situ* measurements (outside the lab), providing fast analysis and requiring small amounts of reagents, minimizing waste production [12–16]. Some work has been reported describing the development of μ PADs for copper determination in water samples [17–22]. However, these works involve wax (or inkjet) printing procedures for the μ PAD assembly, which results in a more expensive and environmentally harmful process due to the use of wax with costly consumables and an extra step of heating (high temperatures between 120 °C and 200 °C). To overcome these disadvantages, a new paper device for copper determination in water is proposed in this work, without the use of wax or inkjet printing procedures, resulting in a more cost-effective, environmentally

* Corresponding author.

E-mail address: rmesquita@ucp.pt (R.B.R. Mesquita).

<https://doi.org/10.1016/j.talanta.2024.125683>

Received 30 October 2023; Received in revised form 12 January 2024; Accepted 15 January 2024

Available online 24 January 2024

0039-9140/© 2024 The Authors. Published by Elsevier B.V. This is an open access article under the CC BY-NC-ND license (<http://creativecommons.org/licenses/by-nc-nd/4.0/>).

friendly, and simpler assembly process.

A rhodamine-based chelator – Mod-RHOB (Fig. 1) with enhanced affinity and selectivity to form a strong complex with copper(II) was used in this work. Although rhodamines belong to an important class of fluorescent molecules widely used as fluorescent markers, particularly in biomedical applications such as biotechnology and medical imaging [23,24] to maintain the fluorescent lighting conditions for image analysis would be a challenge in “outside the lab” approach. So, the Mod-RHOB chelator used in this work, not only exhibits fluorescent properties but also forms a coloured complex with copper(II). Hence, it was used as a chromogenic reagent for colorimetric detection, changing from colourless (absence of Cu^{2+}) to pink (presence Cu^{2+}).

The proposed work describes the development of a μPAD for *in-situ* copper determination in natural waters, using the previously synthesized Mod-RHOB chelator as low-toxicity reagent to ensure an environmentally friendly approach. The developed device offers a practical and effective tool for monitoring water quality across various types of water samples, including seawater samples.

2. Material and methods

2.1. Reagents and solutions

All the solutions were prepared with analytical grade chemicals and Milli-Q water (resistivity $\geq 18 \text{ M}\Omega \text{ cm}$, Millipore, Bedford, MA, USA).

Mod-RHOB chelator was synthesized from Rhodamine B through a two-step procedure (see Electronic Supplementary Material for details) and all the reagents used were acquired from Sigma-Aldrich (Germany). In the first step, rhodamine B hydrazide was synthesized using a procedure previously reported by our group [25]. To this process, rhodamine B, excess of hydrazine hydrate and ethanol were mixed, and the reaction was promoted by microwave digestion during 20 min at 80°C . After cooling to room temperature and evaporation of the solvent, the obtained solid was washed prior to the second step (see Electronic Supplementary Material Fig. 1). The second step was performed following the procedure reported in a previous work [26]. A solution of the produced solid, rhodamine B hydrazide, was mixed with phenylene 1,4-diisothiocyanate and tetrahydrofuran (THF) and left to react for 5, then the solvent was evaporated and the obtained solid purified (see Electronic Supplementary Material Fig. 2).

The reagent stock solution was daily prepared by dissolving approximately 2 mg of Mod-RHOB powder in 100 μL of 99.9 % dimethyl sulfoxide solution (DMSO, Sigma-Aldrich, Germany), corresponding to a final concentration of 20 g L^{-1} . The Mod-RHOB solution used in the μPAD was a dilution of the 20 g L^{-1} in ethanol absolute (Scharlau, Spain), resulting in a final concentration of 0.50 g L^{-1} .

The hydrogen carbonate buffer solution at pH 9 was prepared dissolving 3.4 g of NaHCO_3 (Merck, Germany) in 50 mL of water to attain a final concentration of 0.8 mol L^{-1} [27].

A copper stock solution of 5.00 g L^{-1} was prepared by dissolution of

2 g of CuSO_4 (Panreac, Germany) in 100 mL of water. An intermediate solution of 5.0 mg L^{-1} was obtained by dilution and used to prepare the working standards in range $0.050\text{--}0.50 \text{ mg L}^{-1}$.

Artificial seawater was prepared according to Kester et al. (1967) [28], to the final composition of: 23.9 g L^{-1} of NaCl (Merck, Germany), 4.01 g L^{-1} of Na_2SO_4 (Merck, Germany), 0.677 g L^{-1} of KCl (Merck, Germany), 0.196 g L^{-1} of NaHCO_3 (Merck, Germany), 0.098 g L^{-1} of KBr (Merck, Germany), 0.026 g L^{-1} of H_3BO_3 (Aldrich, USA), 0.003 g L^{-1} of NaF (Merck, Germany), 10.84 g L^{-1} of $\text{MgCl}_2 \cdot 6\text{H}_2\text{O}$ (Merck, Germany), 1.50 g L^{-1} of $\text{CaCl}_2 \cdot 2\text{H}_2\text{O}$ (Merck, Germany), and 0.0027 g L^{-1} of $\text{SrCl}_2 \cdot 6\text{H}_2\text{O}$ (Sigma, USA). The proper amount of all the listed solids was dissolved in 1 L of water.

The solutions used in the interference studies were prepared from the respective solids: $\text{CaCl}_2 \cdot 2\text{H}_2\text{O}$ (Sigma, USA); $\text{MgCl}_2 \cdot 6\text{H}_2\text{O}$ (Merck, Germany); $\text{ZnSO}_4 \cdot 7\text{H}_2\text{O}$ (Sigma, USA); $\text{Al}_2(\text{SO}_4)_3$ (Merck, Germany); $\text{CoSO}_4 \cdot 7\text{H}_2\text{O}$ (Merck, Germany); $\text{MnCl}_2 \cdot 2\text{H}_2\text{O}$ (Merck, Germany); $\text{Fe}_2(\text{SO}_4)_3 \cdot \text{H}_2\text{O}$ (Riedel-de-Haen); NiCl_2 (Sigma, USA).

2.2. μPAD assembly

The assembly of the developed microfluidic device consisted in aligning three filter paper discs with 9.5 mm diameter in twenty-four hydrophilic units (6 columns x 4 rows distribution). These units correspond to the μPAD hydrophilic zone and the plastic laminating pouch (Q-connect, $75 \times 110 \text{ mm}$, glossy, $125 \mu\text{m}$), where they units placed, creates the hydrophobic zone after lamination.

The three layers that compose each paper unit (Fig. 2A) correspond to: a top layer, the reagent layer (R layer), consisting of Whatman 42 filter paper discs; a middle layer, the buffer layer (B layer) consisting of Whatman 1 filter paper discs; and a bottom layer, an empty layer (E layer), consisting of Whatman 3 filter paper discs. The paper discs for the R layer were prepared adding $12 \mu\text{L}$ of Mod-RHOB ligand solution to each disc and oven dry at 50°C for 10 min. The paper discs for the B layer were prepared adding $10 \mu\text{L}$ of buffer solution to each disc and oven dry at 50°C for 10 min.

After manually aligning the twenty-four paper units under the previously perforated 3 mm holes of the plastic pouch top sheet (L_1), the μPAD hydrophobic zone was established by the lamination process. This process was conducted using a laminator (United Office – ULG 300 B1, Germany) that maintained a constant temperature of approximately 60°C . The lamination process both sheets of the plastic pouch (L_1 and L_2) are sealed together creating a physical separation between the different hydrophilic paper units.

2.3. Copper(II) quantification

For the copper determination, on the assembled μPAD , $20 \mu\text{L}$ of standard/sample was loaded through the sample holes, which was absorbed in approximately 2 min. The reaction between the Mod-RHOB and copper forms a pink complex in the R layer which becomes more intense with increasing copper concentration (Fig. 2B).

Five minutes after loading the standard/sample, the top layer of the μPAD , corresponding the detection zone, was scanned using a flatbed scanner (Canon CanoScan LIDE 300, Japan). The intensity of the coloured complex was measured using an image software (ImageJ, National Institutes of Health, USA). The acquired high-resolution image was processed applying a RGB stacking, and the intensity readings were acquired using the green filter, as complementary colour of the formed pink product. For each detection unit, the measurement area was set to correspond to the μPAD sample hole ($3 \text{ mm} = 90 \times 90 \text{ pixels}$). The intensity values were converted into absorbance values using the equation: $A = \log_{10} I_0 / I_S$ where I_0 is the average of the blank intensities ($n = 4$) and I_S is the intensity of the standard/sample signal. A calibration curve was then established, correlating the average absorbance values ($n = 4$) obtained for each copper standard concentration, and used to

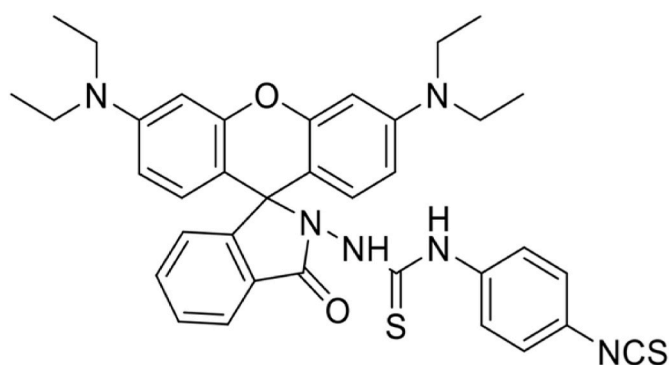


Fig. 1. Formula of Mod-RHOB chelator.

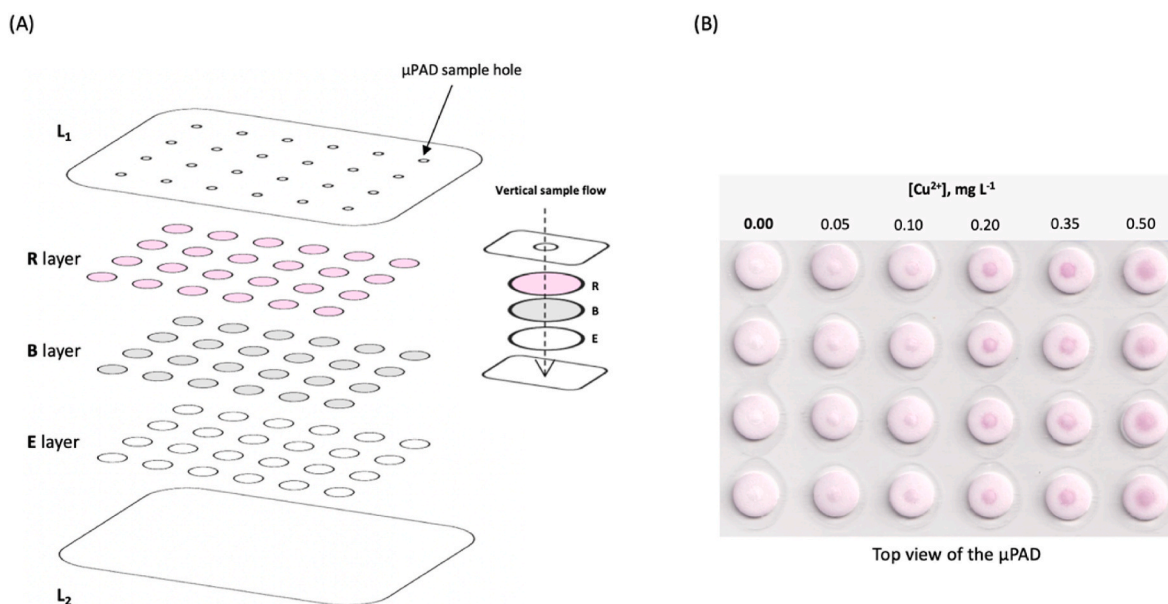


Fig. 2. Schematic representation of the μ PAD assembly for copper determination in waters: (A) Paper discs alignment and the respective μ PAD layers: L_1 and L_2 , laminating pouches sheets; R layer, reagent layer; B layer, buffer layer; E layer, empty layer; (B) Real image of the μ PAD detection zone after loading the copper standard solutions.

interpolate the average absorbance ($n = 4$) obtained from water samples.

2.4. Sample collection

Several water samples from different sources, namely tap water, well water, river water and seawater, were collected in plastic bottles with 500 mL capacity and kept refrigerated at 4 °C until used. The samples were directly applied in the developed μ PAD, with no other treatments. The physical-chemical parameters of the water samples used in the accuracy assessment and recovery studies were listed, namely, pH and conductivity (see Electronic Supplementary Material Table 1).

2.5. Accuracy assessment

The accuracy of the developed μ PAD for copper determination, was attained analysing the collected waters (estuarine and well waters) with the developed device and comparing the results with the results obtained using Inductively Coupled Plasma – Optical Emission Spectrometer (ICP-OES), in a PerkinElmer Optima 7000 dv (USA) equipment. For the ICP-OES determination, the water samples were diluted so that its concentration would fit within the linear range of the corresponding calibration curves ($10\text{--}100 \mu\text{g L}^{-1}$) and acidified with nitric acid to obtain a final concentration of 0.7 mol L^{-1} .

Additionally, recovery percentages studies were carried out for several types of waters, namely tap, river, harbour, and seawater.

3. Results and discussion

The developed work aimed for copper quantification in different types of water, using the colour reaction with Mod-RHOB chelator. Since it was the first time that the Mod-RHOB was used as colour reagent in a μ PAD, several physical and chemical parameters affecting the formation of the colour complex were studied to obtain the highest sensitivity. The μ PAD operation parameters optimization studies were performed by comparing the slope of the calibration curves, using copper standards solutions within the concentration range of $50.0\text{--}500 \mu\text{g L}^{-1}$.

3.1. Preliminary studies - Mod-RHOB chelator

Mod-RHOB solubility was tested in different solvents, namely water, ethanol, and dimethyl sulfoxide (DMSO). These tests were performed by visual observation when trying to dissolve 2 mg in 100 μL . DMSO was the only solvent that provided a total dissolution. The challenge became to dry the paper discs, at the oven temperature usually used (about 50 °C) considering that DMSO has a high boiling point (about 189 °C). So, a 99.9 % DMSO solution was used to prepare several dilutions in water with the aim of reducing the DMSO amount. The percentage of DMSO (from 1 to 40 %) at the set drying time (10 min) were tested by loading 15 μL of each percentage of DMSO solutions in paper discs and dried at 50 °C in the oven (see Electronic Supplementary Material Fig. 3). The papers discs with 10 % or less of DMSO were the only ones that dried within 10 min. However, when the Mod-RHOB solution was prepared with 10 % of DMSO and 90 % of water, the colour solution presented suspensions. Then, the solvent for the dilution of the stock chelator solution was also evaluated and different solvents were tested, namely water, hydrogen carbonate buffer and ethanol. Ethanol was the chosen solvent because it was the only that provided a homogenous solution.

After setting the Mod-RHOB chelator solution preparation, a first paper-based approach was made. Based upon a previous work with metal ions chelators, a similar design was set [15]. A three layer μ PAD was established having the reagent solution in the top layer of the μ PAD. Then, targeting *in-situ* water analysis, the need for the buffer solution was evaluated, to be placed at the second layer of the three-layer assembly. For this study, two calibration curves were made, one with buffer solution in the second layer and one without, and the higher sensitivity was obtained with buffer solution, so that was the chosen option (see Electronic Supplementary Material Fig. 4). The choice of having a buffer solution in the second layer also ensures a constant reaction pH.

3.2. Reagent layer optimization

The first physical parameter to be studied was the paper porosity of the reagent layer. Calibration curves were established using filter papers with three pore sizes: 2.5 μm (Whatman 5, W5), 11 μm (Whatman 1,

W1) and 20–25 μm (Whatman 4, W4). According to the results obtained (Fig. 3A), the paper with the lowest porosity (W5) showed the highest sensitivity, so the chosen porosity was 2.5 μm .

Then, different types of filter paper (with similar porosity of 2.5 μm) were tested: qualitative (Whatman 5, W5), ashless (Whatman 42, W42), hardened low ash (Whatman 50, W50) and hardened ashless (Whatman 542, W542). Comparing the calibration curve slopes (Fig. 3B), the sensitivities were very similar, except using W42 filter paper which showed a slightly higher sensitivity so, it was the one chosen.

Afterwards, the concentration of the Mod-RHOB was studied within the range of 0.1–2.5 g L^{-1} establishing calibration curves for each concentration (Fig. 3C). There was not a significant difference in sensitivity, except for the Mod-RHOB concentration of 0.1 g L^{-1} that presented the lowest sensitivity (slope deviation >10 %). So, 0.5 g L^{-1} was the Mod-RHOB concentration that was chosen, as a compromise between sensitivity and reagent consumption.

We chose to use a volume of 12 μL for the Mod-RHOB solution because it is the maximum volume that the 9.5 mm paper disc can support without overflowing. By using this volume, we ensure that we have over 30 times the reagent amount necessary for the reaction. Higher volumes of the reagent solution were not tested because they either resulted in overflow.

3.3. Buffer layer optimization

The buffer layer corresponds to the middle layer of the μPAD unit, and so the paper type was set for qualitative paper as a more economical choice. In this context, only the paper porosity was tested using the same porosities as those tested in the reagent layer: 2.5 μm (W5), 11 μm (W1) and 20–25 μm (W4). The calibration curve slopes obtained with each paper were compared (see Electronic Supplementary Material Fig. 5A). There were no significant differences in sensitivity between W5 and W1, while the paper with the higher porosity (W4) presented the lowest sensitivity (slope deviation >10 %). Whatman 1 (W1) was the filter paper chosen because it provided a faster sample absorption time (\approx 5 min).

Loading the W1 paper disc with different volumes of NaHCO_3 buffer solution was tested and volumes from 5 to 12 μL were used, representing the minimum and maximum volume possible, respectively. According to the results obtained (see Electronic Supplementary Material Fig. 5B), 10 μL was the lowest volume that provided the highest sensitivity.

3.4. Sample volume and sample hole size

The sample volume is a key parameter to enable the lowest detection

limit possible. So, the sample volume ranging from 20 to 35 μL was tested (Fig. 4A). As the sample volume increased, the sample absorption time also increased: 2–25 min, respectively. Surprisingly, the increase of the sample/standard volume did not result in an increase of sensitivity, with the lowest volume tested presenting the highest sensitivity. Although the increase of sample/standard volume is expected to result in a higher absorbance signal as there is a higher amount to react, some dispersion through the reagent paper layer could result in an opposite effect. In the end, 20 μL was the volume chosen, providing a faster analysis time.

The diameter of the μPAD sample hole was also studied because it was directly related to the sample absorption time and the intensity of the coloured product area. When diameters between 2 and 6 mm were tested (Fig. 4B), it was possible to conclude that by increasing the diameter, the sample absorption time, and the intensity of the coloured product decreased. The slope of each calibration curve was compared (Fig. 4C), and 3 mm was the diameter that was chosen as a compromise between sensitivity and sample absorption time.

3.5. Stability assessment

Stability studies were performed not only to evaluate the potential degradation of the Mod-RHOB solution (before μPAD assembly), but also to study the stability of the coloured product formed (after placing the water samples) and the stability of the μPAD storage (before being used).

3.5.1. Reagent stability

The stability studies of the Mod-RHOB solutions were performed because it was possible to observe that the colour of both Mod-RHOB solutions (stock solution in DMSO and working solution with ethanol) varied with time. The stability assessment was made for both solutions separately: stock solution of Mod-RHOB in DMSO (see Electronic Supplementary Material Fig. 6A) and working solution of Mod-RHOB in ethanol (see Electronic Supplementary Material Fig. 6B).

The stability of the Mod-RHOB stock solution (in DMSO) was made preparing one stock solution and making the working solution (dilution in ethanol) on different days from 1 day up to 7 days (1 week). For the stability of the Mod-RHOB working solution, calibration curves were set in consecutive days (1–7 days) using the same solution. According to the results obtained, both Mod-RHOB solutions were stable only for up to 2 days.

3.5.2. Stability of the coloured product

Since one of the main advantages of microfluidic devices is

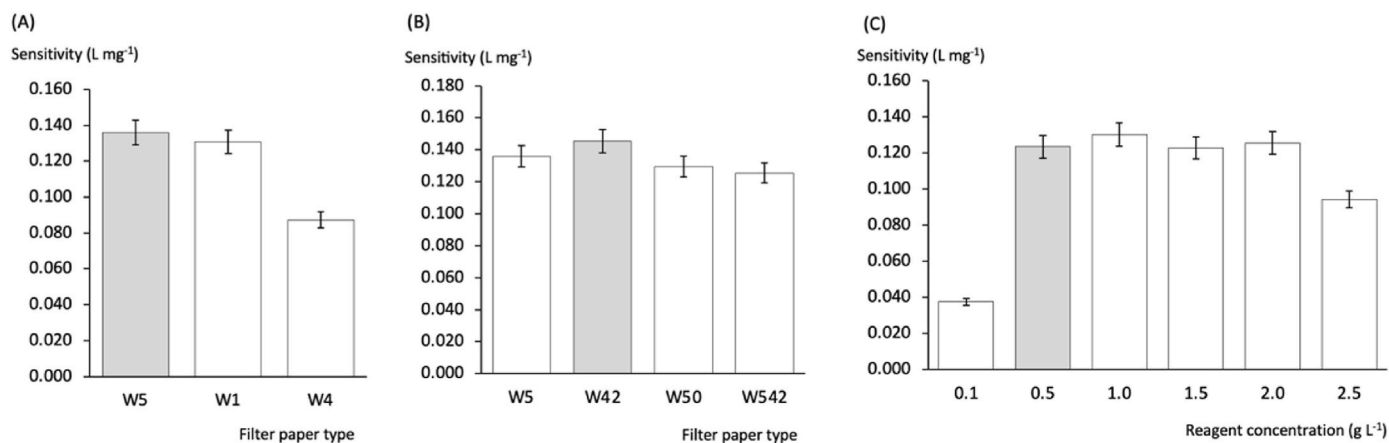


Fig. 3. Study of the influence in the calibration curve slope of different filter papers and different concentrations of Mod-RHOB in the reagent layer: (A) papers with different pore sizes; (B) different types of filter papers and (C) different reagent concentrations; the grey bars represent the chosen option; the error bars represent 10 % deviation of the measurements.

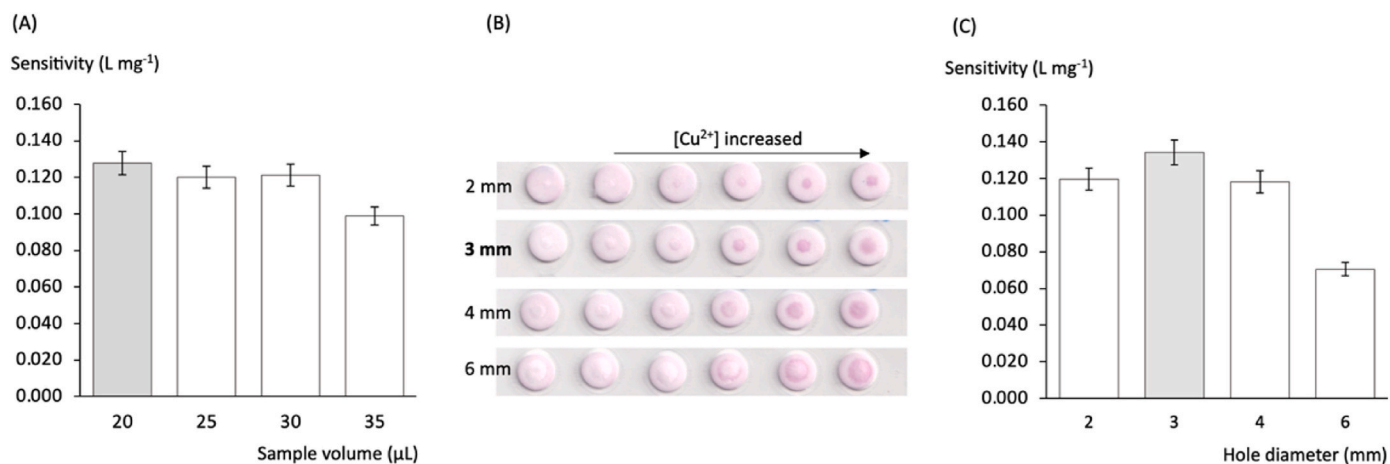


Fig. 4. Study of the influence in the calibration curve slope by different sample/standard volumes (A); study of the influence on the colour complex area by using different diameters (2, 3, 4 and 6 mm) for the μ PAD sample hole (B); study of the influence in the calibration curve slope by using different sample hole diameters (C); the grey bars represent the chosen option; the error bars represent 10 % deviation of the measurements.

portability, allowing an *in-situ* water analysis, it was very important to evaluate the stability of the coloured product after placing the water sample. For this study, a calibration curve for copper determination was prepared and the μ PAD detection zone was scanned several times (up to 70 min). According to the results obtained (see Electronic Supplementary Material Fig. 7), no significant differences in sensitivity were observed (slope deviation <10 %) up to 30 min. In an attempt to increase the scanning time, a new μ PAD was prepared where, after applying the sample, the μ PAD sample holes were covered with adhesive tape. However, no significant differences were also observed up to 30 min, with or without adhesive tape. Therefore, the sensitivity of the coloured complex was stable if the detection zone reading took up to 30 min.

3.5.3. μ PAD stability

To study the stability of the developed μ PAD (before the sample loading), several devices were prepared and stored closed in sealed plastic bags under different atmospheric conditions: in contact with air and in vacuum. For both atmospheric conditions, the μ PADs were stored at room temperature (approximately 21 °C), exposed to light, and protected from light (covered with aluminium foil). Additionally, some devices in vacuum atmospheric conditions were also stored in a refrigerator (approximately 5 °C), exposed, and protected from light.

Different time periods were tested, ranging from 24 h to 1 month (Fig. 5). For each storage period and condition, a calibration curve was set with the stored μ PAD and compared with a calibration curve of freshly prepared μ PAD (fresh CC in Fig. 5).

As shown in Fig. 5, there was not statistical differences in sensitivity up to 1 month of storage between the fresh calibration curve and the μ PADs stored in vacuum conditions, in the refrigerator and protected from light. This was also observed in the calibration curve slope related with the μ PADs stored in vacuum conditions at room temperature, protected from light, but only up to 2 weeks. So, 1 month was the maximum storage time of μ PAD lifetime.

3.6. Interference assessment

3.6.1. Potential interfering metal ions

Although the Mod-RHOB chelator has a higher affinity towards copper, it was important to assess the potential interference of some bivalent and trivalent cations that can also be present in water. The interfering species and corresponding concentrations tested in this study were based on the maximum values reported in international legislation. Copper standards with a concentration of 0.25 mg L⁻¹ were prepared with different concentrations of the potential interfering ions. The absorbance values of the copper standard with ($A_{Cu\&Interf}$) and without

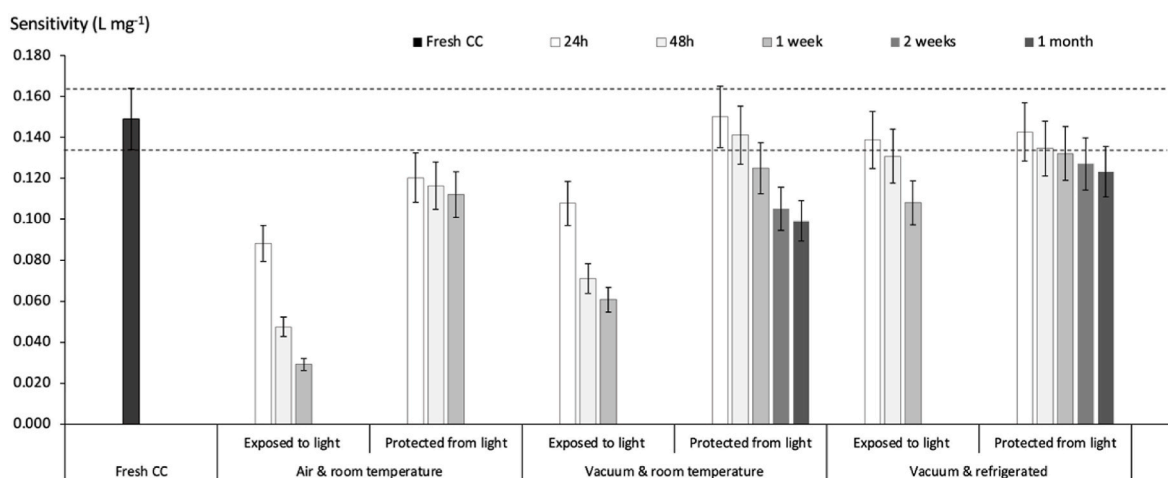


Fig. 5. Study of the stability of the developed μ PAD under different storage conditions. The black bar represents the average of five calibration curves and the black dashed horizontal lines represent the range of the error bars with 10 % deviation from average of the calibration curves. The grey bars indicate the different storage times. The error bars represent 10 % deviation of the measurements.

Table 1

Assessment of possible interfering ions in the determination of copper according to international legislation values; UNFAO, United Nations Food and Agriculture Organization; EPA, Environmental Protection Agency.

Possible interfering ion	Legislation maximum values (mg L ⁻¹)	Interference (%)
Ca ²⁺	15 ^a	-6.3
Mg ²⁺	5.0 ^b	+2.9
Zn ²⁺	0.1 ^b	-3.6
Al ³⁺	1.0 ^c	-3.0
Co ²⁺	0.1 ^a	+1.4
Mn ²⁺	0.2 ^a	+0.8
Fe ³⁺	5.0 ^b	+4.6
Ni ²⁺	0.2 ^a	-1.2

^a UNFAO.

^b groundwater.

^c EPA – drinking water.

(A_{Cu}) the potential interfering ion were registered, and the interference percentage calculated (Table 1). The interference percentage was calculated according to the equation: Interference % = [(A_{Cu&Interf} - A_{Cu})/(A_{Cu})]. No significant interferences (Interference% < 10 %) were observed for all the tested metal ions expected in the water samples.

3.6.2. Seawater matrix

One of the main objectives of this work was develop a device that would allow analysing different types of water samples, namely tap, well and river water as well as seawater. So, copper standards with the same concentration range were prepared in artificial seawater and a calibration curve was set. When comparing the calibration curve slopes of copper standards prepared in water and seawater (see Electronic Supplementary Material Fig. 8), it was possible to observe that the calibration curve slope of copper standards in seawater decreased by approximately 40 %. This can be explained by the lower availability (thus activity) of the copper ions in a saline matrix.

3.7. Analytical features of the developed μ PAD

After all the studies performed for the copper determination based on the coloured complex formed with Mod-RHOB, the analytical

Table 2

Summary of the analytical features of the developed μ PAD for copper determination in water; SD, standard deviation; LOD, limit of detection; LOQ, limit of quantification.

Targeted sample	Dynamic range (mg L ⁻¹)	Calibration curve ^a A = Slope \pm SD [Cu ²⁺] + Intercept \pm SD	LOD (μ g L ⁻¹)	LOQ (μ g L ⁻¹)	Reagent consumption per μ PAD
Fresh water	0.05–0.50	A = 0.152 \pm 0.014 [Cu ²⁺] + 0.002 \pm 0.001 R ² = 0.998 \pm 0.002	10	34	0.144 mg of ligand 1.20 mg of NaHCO ₃
Seawater	0.10–0.50	A = 0.069 \pm 0.002 [Cu ²⁺] - 0.002 \pm 0.001 R ² = 0.996 \pm 0.003	28	92	

^a n = 5.

Table 3

Accuracy assessment; analysis results of several water samples using the newly developed μ PAD method for copper determination; SD, standard deviation (n = 4); RE, relative error.

Sample type	Sample ID	Reference Method (ICP-OES) [Cu ²⁺] \pm SD, mg L ⁻¹	μ PAD Method [Cu ²⁺] \pm SD, mg L ⁻¹	RE (%)
Well water	W1	0.088 \pm 0.001	0.087 \pm 0.006	-1.1
	W2	0.061 \pm 0.002	0.062 \pm 0.017	+1.6
	W3	0.103 \pm 0.003	0.104 \pm 0.011	+1.0
Estuary water samples	E1	0.143 \pm 0.002	0.138 \pm 0.034	-3.5
	E2	0.251 \pm 0.001	0.247 \pm 0.023	-1.6
	E3	0.143 \pm 0.003	0.142 \pm 0.006	-0.7
	E4	0.114 \pm 0.002	0.118 \pm 0.017	+3.5
	E5	0.054 \pm 0.001	0.052 \pm 0.016	-3.7

A linear regression was established (see Electronic Supplementary Material Fig. 9) between the two sets of results: [Cu²⁺] _{μ PAD} = 0.978 (\pm 0.016) [Cu²⁺]_{ICP-OES} + 0.002 (\pm 0.002), where the values in parenthesis are 95 % confidence limits.}}

characteristics of developed microfluidic paper-based were summarized in Table 2.

Two calibration curves for copper determination, in fresh waters and seawater, were obtained according to the copper standards used (ESM Fig. 8). The limit of detection (LOD) and the limit of quantification LOQ, were calculated according to the International Union of Pure and Applied Chemistry (IUPAC) recommendations [29], as three and ten times, respectively, the standard deviation of the average of the intercept (n = 5) divided by the calibration curve slope average. The dynamic range of the developed method was established based on the calculated LOQ and up to the limit of the linear response.

The repeatability of the method was assessed by calculating the relative standard deviation (RSD) based upon the copper concentration average obtained for a river water sample using 10 measurements (RSD = 2.1 %). Additionally, the interday reproducibility was calculated as the RSD of the slope (RSD_{interday} = 1.4 %) calculated from five calibration curves on consecutive days.

The reagent consumption was calculated for one μ PAD (24 paper discs units): 0.144 mg of Mod-RHOB and 1.20 mg of hydrogen carbonate. The sample consumption was calculated per determination as 80 μ L (20 μ L of sample per reading unit and four paper units per determination).

3.8. Application to natural waters

3.8.1. Accuracy assessment

For the accuracy assessment, eight water samples were analysed with the developed microfluidic device, and the results were compared with the results obtained by the reference procedure of the ICP-OES measurements (Table 3).

The linear correlation showed that the estimated slope and intercept do not differ statistically from values 1 and 0, respectively. Therefore, it was possible to conclude that the two sets of results were not statistically different.

3.8.2. Recovery studies

Additionally, for further accuracy assessment, recovery studies were also performed using several types of water samples. The samples were

Table 4
Recovery percentages calculated from spiked natural waters assessed with the developed method.

Sample type	[Cu ²⁺] _{Initial} (µg L ⁻¹)	Sample ID	[Cu ²⁺] _{Added} (mg L ⁻¹)	[Cu ²⁺] _{Found} ± SD (mg L ⁻¹)	Recovery %
Tap water (T#)	<10	T1	0.100	0.104 ± 0.014	104
			0.300	0.291 ± 0.020	97.1
			0.100	0.102 ± 0.013	102
River water (R#)	<10	R1	0.300	0.323 ± 0.016	108
			0.100	0.097 ± 0.003	97.1
			0.300	0.310 ± 0.016	103
			0.100	0.096 ± 0.006	95.6
Harbour (H#)	<10	H1	0.300	0.287 ± 0.011	95.7
			0.100	0.095 ± 0.011	95.1
			0.300	0.298 ± 0.027	99.4
Seawater (S#)	<10	S1	0.100	0.106 ± 0.015	106
			0.300	0.310 ± 0.026	103
			0.100	0.104 ± 0.017	104
			0.300	0.315 ± 0.024	105

spiked with different volumes of a 5.0 mg L⁻¹ copper standard to final concentrations of 0.10 and 0.30 mg L⁻¹. Then, the recovery percentages were calculated according to the IUPAC recommendations [30]: Recovery % = $\frac{([Cu^{2+}]_{Found} - [Cu^{2+}]_{Initial})}{[Cu^{2+}]_{Added}} \times 100$; when the [Cu²⁺]_{Initial} is below LOD, the formula becomes: Recovery % = $\frac{[Cu^{2+}]_{Found}}{[Cu^{2+}]_{Added}} \times 100$ (Table 4).

The overall average was 101 % with a relative standard deviation of 4.3 %. A statistical test (*t*-test) was used to evaluate if the mean recovery value did significantly differ from 100 %. With a 95 % significance level, the calculated *t*-value was 0.149 with a correspondent critical value of 2.53. The statistical results indicate the absence of multiplicative matrix interferences.

Furthermore, because different natural waters were used, it confirmed that the developed method was applicable to different types of water samples.

4. Conclusions

In summary, we have successfully developed a new microfluidic paper-based analytical device for the quantification of copper in water. This paper device, in combination with a low-toxicity chelator, Mod-RHOB, represents a ground-breaking technique as it allows the measurement of copper levels in several types of water, including seawater samples.

The developed µPAD has demonstrated exceptional affinity and specificity for copper, exhibiting a colorimetric response by forming a coloured complex from light pink (absence of Cu²⁺) to dark pink

(presence of Cu²⁺). This µPAD was also shown to be effective, portable, and disposable, providing a rapid on-hand measurement, in a more economical way compared to conventional techniques for water monitoring. With our new approach, we have achieved a dynamic concentration range of 0.05–0.50 mg L⁻¹, with low quantification limits, namely 34 µg L⁻¹. Furthermore, the device remains stable for up to one month when stored in vacuum conditions and refrigerated while being protected from light. Once the sample is loaded, the colorimetric response can be scanned for up 30 min, allowing ample time for analysis. The analytical features of the developed paper device were compared with those reported in other studies for copper determination (Table 5). This work presented similar or even lower limits of detection and proved to be an innovative and more environmentally-friendly approach, offering a reliable tool for water analysis in various environments.

In the pursuit of developing innovative technologies, the choice of appropriate tools is essential to evaluate the environmental sustainability of the system. In this context, the application of the RGB additive colour model [31] and the GREENness calculator [32] was used as an analytical metric which offers a valuable framework for assessing the environmental impact of the µPAD system. When the RGB model was used, the result was “white” (93.6 %). The RGB additive colour model represents three main attributes of the evaluated method: analytical performance – R (Red), safety/eco-friendliness – G (Green) and productivity/practical effectiveness – B (Blue). The results of the RGB model can be interpreted as: white colour (mix of three primary colours) means that all primary attributes have a satisfactory degree; secondary colours (magenta, yellow or cyan) if the method is satisfactory in terms of two

Table 5
Comparison of the analytical characteristics of developed µPAD and other copper paper devices; ND, not documented.

[Cu ²⁺] range (mg L ⁻¹)	LOD (µg L ⁻¹)	Sample volume (µL)	Type of water	µPAD assembly	Image Processing	Observations	Year	Reference
0.05–0.50	10	20 µL	Tap, well, river and seawater	Cut paper disks inserted into a laminated plastic pouch	ImageJ software	Vertical flow; Applied to different types of water samples, including seawater.	–	This work
0.064–0.44	22	400 µL	Natural water	Wax printing method; Heating at 120 °C	Photoshop software; ICS-1100; IC-UV	Use of a SPE column as a pre-treatment method	2023	[17]
0.10–30	60	19.2 µL	Natural and wastewater	Inkjet printing method	ImageJ software	Use of a polymer inclusion membrane (PVC)	2013	[18]
0.0005–0.2	0.3	20 µL	Drinking and groundwater	Wax printing method; heating at 175 °C	ImageJ software	Semi-quantitative determination	2015	[19]
1.0–6.0	ND	20 µL	Drinking water	Wax printing technique; heating at 150 °C	Cu ²⁺ determination using a ruler printed directly on the device	Semi-quantitative determination using a distance-based paper analytical device	2017	[20]
0.02–500	ND	20 µL	Drinking water	Wax printing method	ImageJ software	Solid-phase extraction (sample pre-treatment) coupled to a paper-based technique	2018	[21]
0.32–63.55	320	300 µL	Tap and pond water	Wax printing method; heating at 200 °C	ImageJ software	Use of several toxic reagents	2021	[22]

attributes; primary colours (red, green or blue) if it has only one attribute and lacks the other two; grey colour means that the method utilization may be considered. The obtained final score of 0.94 on the GREENness calculator indicates a strong alignment with sustainable practices, suggesting that the developed μ PAD presents favourable attributes in terms of minimizing its ecological footprint. The GREENness assessment is based on 12 principles of green analytical chemistry and is transformed into a unified 0–1 scale: a score of 0 would typically represent a complete absence of green principles and a score of 1 signifies full adherence to green principles. In the GREENness calculator, it was not possible to include the Mod-RHOB chelator as the reagent, but these ligands have low toxicity since they are used as fluorescent markers in biomedical applications.

CRedit authorship contribution statement

Juliana I.S. Aguiar: Formal analysis, Investigation, Validation, Writing – original draft, Methodology. **Susana O. Ribeiro:** Formal analysis, Investigation, Methodology. **Andreia Leite:** Funding acquisition, Project administration, Resources, Writing – review & editing. **Maria Rangel:** Conceptualization, Resources, Writing – review & editing. **Antônio O.S.S. Rangel:** Conceptualization, Funding acquisition, Resources. **Raquel B.R. Mesquita:** Conceptualization, Data curation, Investigation, Project administration, Writing – review & editing.

Declaration of competing interest

The authors declare that they have no known competing financial interests or personal relationships that could have appeared to influence the work reported in this paper.

Data availability

Data will be made available on request.

Acknowledgment

A. Leite thanks FCT/MCTES (Fundação para a Ciência e Tecnologia and Ministério da Ciência, Tecnologia e Ensino Superior) for funding through program DL 57/2016 – Norma transitória. This work received financial support from National Funds FCT/MCTES, under the Partnership Agreement PT2020 through project PTDC/QUI-QIN/28142/2017. Additionally, the research team would like to thank FCT for the projects 2022.08713.PTDC NORTE-07-0162-FEDER-000048, UIDB/50016/2020, UIDB/50006/2020 and UIDP/50006/2020.

Appendix A. Supplementary data

Supplementary data to this article can be found online at <https://doi.org/10.1016/j.talanta.2024.125683>.

References

- R. Manne, M.M.R.M. Kumaradoss, R.S.R. Iska, A. Devarajan, N. Mekala, Water quality and risk assessment of copper content in drinking water stored in copper container, *Appl. Water Sci.* 12 (2022) 27, <https://doi.org/10.1007/s13201-021-01542-x>.
- E.C. Emenike, A.G. Adeniyi, P.E. Omuku, K.C. Okwu, K.O. Iwuozor, Recent advances in nano-adsorbents for the sequestration of copper from water, *J. Water Proc. Eng.* 47 (2022), <https://doi.org/10.1016/j.jwpe.2022.102715>.
- S. Lunvongsa, T. Tsuboi, S. Motomizu, Sequential determination of trace amounts of iron and copper in water samples by flow injection analysis with catalytic spectrophotometric detection, *Anal. Sci.* 22 (2006) 169–172, <https://doi.org/10.2116/analsci.22.169>.
- A. González, R.B.R. Mesquita, J. Avivar, T. Moniz, M. Rangel, V. Cerdà, A.O.S.S. Rangel, Microsequential injection lab-on-valve system for the spectrophotometric bi-parametric determination of iron and copper in natural waters, *Talanta* 167 (2017) 703–708, <https://doi.org/10.1016/j.talanta.2017.02.055>.
- A. Lace, J. Cleary, A review of microfluidic detection strategies for heavy metals in water, *Chemosensors* 9 (2021) 60, <https://doi.org/10.3390/chemosensors9040060>.
- R.A. Sarvestani, Majid Aghasi, Health risk assessment of heavy metals exposure (lead, cadmium, and copper) through drinking water consumption in Kerman city, Iran, *Environ. Earth Sci.* 78 (2019) 714, <https://doi.org/10.1007/s12665-019-8723-0>.
- T. Jiang, G. Wang, T.H. Chen, Microfluidic particle accumulation for visual quantitation of copper ions, *Mikrochim. Acta* 188 (2021) 176, <https://doi.org/10.1007/S00604-021-04822-0/TABLES/2>.
- J. Paluch, R.B.R. Mesquita, V. Cerdà, J. Kozak, M. Wieczorek, A.O.S.S. Rangel, Sequential injection system with in-line solid phase extraction and soil mini-column for determination of zinc and copper in soil leachates, *Talanta* 185 (2018) 316–323, <https://doi.org/10.1016/j.talanta.2018.03.091>.
- M.I.G.S. Almeida, B.M. Jayawardane, S.D. Kolev, I.D. McKelvie, Developments of microfluidic paper-based analytical devices (μ PADs) for water analysis: a review, *Talanta* 177 (2018) 176–190, <https://doi.org/10.1016/j.talanta.2017.08.072>.
- A.W. Martinez, S.T. Phillips, G.M. Whitesides, Diagnostics for the developing world: microfluidic paper-based analytical devices, *Anal. Chem.* 82 (2010) 3–10, <https://doi.org/10.1021/ac9013989>.
- P. Aryal, E. Brack, T. Alexander, C.S. Henry, Capillary flow-driven microfluidics combined with a paper device for fast user-friendly detection of heavy metals in water, *Anal. Chem.* (2023) 5820–5827, <https://doi.org/10.1021/acs.analchem.3c00378>.
- N. Ansari, N. Trambadiya, A. Lodha, S.K. Menon, A portable microfluidic paper-based analytical device for blood detection and typing assay, *Aust. J. Forensic Sci.* 53 (2021) 407–418, <https://doi.org/10.1080/00450618.2020.1740321>.
- J.I.S. Aguiar, M.T.S. Silva, H.A.G. Ferreira, E.C.B. Pinto, M.W. Vasconcelos, A.O.S.S. Rangel, R.B.R. Mesquita, Development of a microfluidic paper-based analytical device for magnesium determination in saliva samples, *Talanta Open* 6 (2022), <https://doi.org/10.1016/j.talo.2022.100135>.
- X. Xiong, J. Zhang, Z. Wang, C. Liu, W. Xiao, J. Han, Q. Shi, Simultaneous multiplexed detection of protein and metal ions by a colorimetric microfluidic paper-based analytical device, *Biochip J* 14 (2020) 429–437, <https://doi.org/10.1007/s13206-020-4407-9>.
- J.I.S. Aguiar, S.O. Ribeiro, A. Leite, M. Rangel, A.O.S.S. Rangel, R.B.R. Mesquita, Iron determination in natural waters using a synthesized 3-hydroxy-4-pyridione ligand in a newly developed microfluidic paper-based device, *Chemosensors* 11 (2023) 101, <https://doi.org/10.3390/chemosensors11020101>.
- A.W. Martinez, S.T. Phillips, M.J. Butte, G.M. Whitesides, Patterned paper as a platform for inexpensive, low-volume, portable bioassays, *Angew. Chem. Int. Ed.* 46 (2007) 1318–1320, <https://doi.org/10.1002/anie.200603817>.
- Q. Wu, J. He, H. Meng, Y. Wang, Y. Zhang, H. Li, L. Feng, A paper-based microfluidic analytical device combined with home-made SPE column for the colorimetric determination of copper(II) ion, *Talanta* 204 (2019) 518–524, <https://doi.org/10.1016/j.talanta.2019.06.006>.
- B.M. Jayawardane, L.D.L.C. Coo, R.W. Cattrall, S.D. Kolev, The use of a polymer inclusion membrane in a paper-based sensor for the selective determination of Cu (II), *Anal. Chim. Acta* 803 (2013) 106–112, <https://doi.org/10.1016/j.aca.2013.07.029>.
- S. Chaiyi, W. Siangproh, A. Apilux, O. Chailapakul, Highly selective and sensitive paper-based colorimetric sensor using thiosulfate catalytic etching of silver nanoparticles for trace determination of copper ions, *Anal. Chim. Acta* 866 (2015) 75–83, <https://doi.org/10.1016/j.aca.2015.01.042>.
- R. Pratiwi, M.P. Nguyen, S. Ibrahim, N. Yoshioka, C.S. Henry, D.H. Tjahjono, A selective distance-based paper analytical device for copper(II) determination using a porphyrin derivative, *Talanta* 174 (2017) 493–499, <https://doi.org/10.1016/j.talanta.2017.06.041>.
- C.W. Quinn, D.M. Cate, D.D. Miller-Lionberg, T. Reilly, J. Volckens, C.S. Henry, Solid-phase extraction coupled to a paper-based technique for trace copper detection in drinking water, *Environ. Sci. Technol.* 52 (2018) 3567–3573, <https://doi.org/10.1021/acs.est.7b05436>.
- P. Kamnoet, W. Aeungmaitrepirom, R.F. Menger, C.S. Henry, Highly selective simultaneous determination of Cu(ii), Co(ii), Ni(ii), Hg(ii), and Mn(ii) in water samples using microfluidic paper-based analytical devices, *Analyst* 146 (2021) 2229–2239, <https://doi.org/10.1039/d0an02200d>.
- C. Queirós, V.A.S. Almodóvar, F. Martins, A. Leite, A.C. Tomé, A.M.G. Silva, Synthesis of novel diketopyrrolopyrrole-rhodamine conjugates and their ability for sensing Cu²⁺ and Li⁺, *Molecules* 27 (2022) <https://doi.org/10.3390/molecules27217219>.
- Q. Zhang, K.M.C. Wong, Photophysical, ion-sensing and biological properties of rhodamine-containing transition metal complexes, *Coord. Chem. Rev.* 416 (2020), <https://doi.org/10.1016/j.ccr.2020.213336>.
- A. Leite, A.M.G. Silva, L. Cunha-Silva, B. De Castro, P. Gameiro, M. Rangel, Discrimination of fluorescence light-up effects induced by pH and metal ion chelation on a spirocyclic derivative of rhodamine B, *Dalton Trans.* 42 (2013) 6110–6118, <https://doi.org/10.1039/c2dt32198j>.
- R.M. Franzini, E.T. Kool, Organometallic activation of a fluorogen for templated nucleic acid detection, *Org. Lett.* 10 (2008) 2935–2938, https://doi.org/10.1021/OL800878B.SUPPL_FILE/OL800878B-FILE003.PDF.
- T. Moniz, C.R. Bassett, M.I.G.S. Almeida, S.D. Kolev, M. Rangel, R.B.R. Mesquita, Use of an ether-derived 3-hydroxy-4-pyridinone chelator as a new chromogenic reagent in the development of a microfluidic paper-based analytical device for Fe (III) determination in natural waters, *Talanta* 214 (2020) 120887, <https://doi.org/10.1016/j.talanta.2020.120887>.

- [28] D.R. Kester, I.W. Duedall, D.N. Connors, R.M. Pytkowicz, Preparation of artificial seawater, *Limnol. Oceanogr.* 12 (1967) 176–179, <https://doi.org/10.4319/lo.1967.12.1.0176>.
- [29] L.A. Currie, Nomenclature in evaluation of analytical methods including detection and quantification capabilities, *Pure Appl. Chem.* 67 (1995) 1699–1723, <https://doi.org/10.1351/pac199567101699>.
- [30] D.T. Burns, K. Danzer, A. Townshend, Use of the terms “recovery” and “apparent recovery” in analytical procedures (IUPAC Recommendations 2002), *Pure Appl. Chem.* 74 (2003) 2201–2205, <https://doi.org/10.1351/pac200274112201>.
- [31] P.M. Nowak, P. Kościelniak, What color is your method? Adaptation of the RGB additive color model to analytical method evaluation, *Anal. Chem.* 91 (2019) 10343–10352, <https://doi.org/10.1021/acs.analchem.9b01872>.
- [32] F. Pena-Pereira, W. Wojnowski, M. Tobiszewski, Agree - analytical GREENness metric approach and software, *Anal. Chem.* 92 (2020) 10076–10082, <https://doi.org/10.1021/acs.analchem.0c01887>.